Evaluation of the MOCAGE chemistry transport model during the ICARTT/ITOP experiment.

N. Bousserez, Jean-Luc Attié, V. H. Peuch, M. Michou, G. Pfister, D. Edwards, L. Emmons, C. Mari, Brice Barret, S. R. Arnold, et al.

Evaluation of the MOCAGE chemistry transport model during the ICARTT/ITOP experiment

N. Bousserez,[1] J. L. Attié,[1] V. H. Peuch,[2] M. Michou,[2] G. Pfister,[3] D. Edwards,[3] L. Emmons,[3] C. Mari,[1] B. Barret,[1] S. R. Arnold,[4] A. Heckel,[5] A. Richter,[5] H. Schlager,[6] A. Lewis,[7] M. Avery,[8] G. Sachse,[8] E. V. Browell,[8] and J. W. Hair[8]

Received 31 May 2006; revised 16 March 2007; accepted 6 April 2007; published 22 May 2007.

[1] Intercontinental Transport of Ozone and Precursors (ITOP), part of International Consortium for Atmospheric Research on Transport and Transformation (ICARTT), was a large experimental campaign designed to improve our understanding of the chemical transformations within plumes during long-range transport (LRT) of pollution from North America to Europe. This campaign took place in July and August 2004, when a strong fire season occurred in North America. Burning by-products were transported over large distances, sometimes reaching Europe. A chemical transport model, Modélisation de la Chimie Atmosphérique Grande Echelle (MOCAGE), with a high grid resolution ($0.5° \times 0.5°$) over the North Atlantic area and a daily inventory of biomass burning emissions over the United States, has been used to simulate the period. By comparing our results with available aircraft in situ measurements and satellite data (MOPITT CO and SCIAMACHY NO_2), we show that MOCAGE is capable of representing the main characteristics of the tropospheric ozone-NO_x-hydrocarbon chemistry during the ITOP experiment. In particular, high resolution allows the accurate representation of the pathway of exported pollution over the Atlantic, where plumes were transported preferentially at 6 km altitude. The model overestimates OH mixing ratios up to a factor of 2 in the lower troposphere, which results in a global overestimation of hydrocarbons oxidation by-products (PAN and ketones) and an excess of O_3 (30–50 ppbv) in the planetary boundary layer (PBL) over the continental United States. Sensitivity study revealed that lightning NO emissions contributed significantly to the NO_x budget in the upper troposphere of northeast America during the summer 2004.

Citation: Bousserez, N., et al. (2007), Evaluation of the MOCAGE chemistry transport model during the ICARTT/ITOP experiment, *J. Geophys. Res.*, *112*, D10S42, doi:10.1029/2006JD007595.

1. Introduction

[2] In recent years, global monitoring from space has offered the unique opportunity to observe intercontinental transport of pollution [*Wilkening et al.*, 2000; *Husar et al.*, 2001; *McKendry et al.*, 2001]. Long-range transport (LRT) events have frequently been observed between Asia and North America [*Jaffe et al.*, 1999; *Fiore et al.*, 2002; *Hudman et al.*, 2004] and between North America and Europe [*Trickl et al.*, 2003; *Auvray et al.*, 2007]. Hemispheric-scale transport has also been reported [*Damoah et al.*, 2004]. During transport, pollution plumes undergo complex chemical transformation. In order to better understand these processes, several field campaigns have been carried out over the last decade, including NARE (North Atlantic Regional Experiment) and OCTA (Oxidising Capacity of the Tropospheric Atmosphere) in 1993 [*Wild et al.*, 1996]. These field experiments have shown that LRT from one continent to another may occasionally influence regional air quality on a downwind continent [*McKendry et al.*, 2001].

[3] Between 1 July and 15 August 2004, in the framework of the ICARTT (International Consortium for Atmospheric Research on Transport and Transformation) project, several scientific teams from Germany, France, the UK and the United States carried out aircraft measurements of chemical species concentrations between N. America and Europe [*Fehsenfeld et al.*, 2006; *Singh et al.*, 2006]. The aim of the ICARTT project, which included smaller national projects such as ITOP (International Transport of Ozone and Precursors) and INTEX-NA (Intercontinental chemical Transport Experiment–North America), was to better un-

[1]Laboratoire d'Aérologie, Université Paul Sabatier, Toulouse, France.
[2]Centre National de Recherches Météorologiques/Météo France, Toulouse, France.
[3]National Center for Atmospheric Research, Boulder, Colorado, USA.
[4]Institute for Atmospheric Science, School of Earth and Environment, University of Leeds, Leeds, UK.
[5]Institute of Environmental Physics, Bremen, Germany.
[6]Institut für Physik der Atmosphäre, Deutsches Zentrum für Luft- und Raumfahrt, Operpfaffenhofen, Wessling, Germany.
[7]Department of Chemistry, University of York, York, UK.
[8]NASA Langley Research Center, Hampton, Virginia, USA.

0148-0227/07/2006JD007595

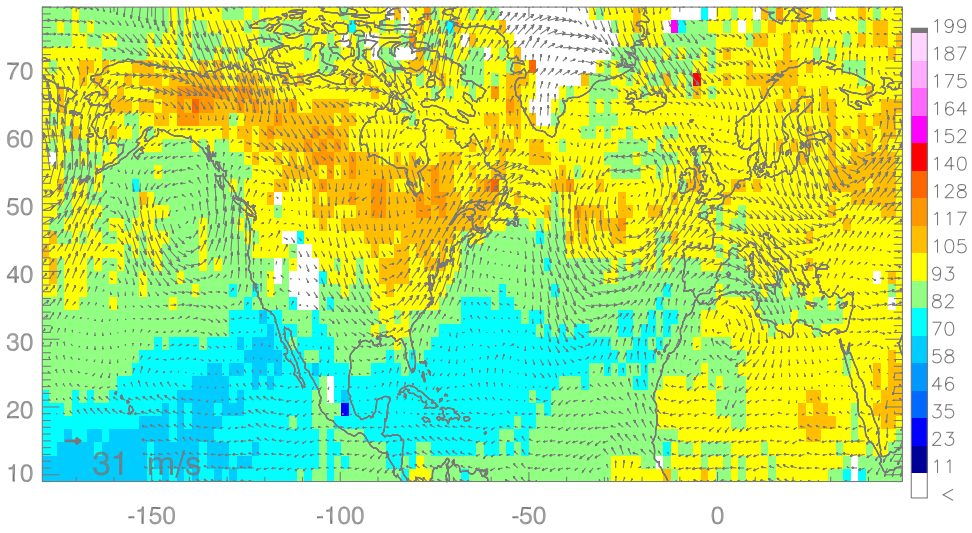

Figure 1. MOPITT CO (ppbv) binned at 2° × 2° and ARPEGE horizontal wind at 500 hPa averaged from 15 July to 15 August 2004.

derstand the mechanisms of pollution chemistry within uplifted air exported from N. America to Europe.

[4] The summer of 2004 was the most severe fire season on record for Alaska and western Canada [*Damoah et al.*, 2006]. Biomass burning inventories estimated that 27 Tg of CO and 0.5 Tg of NO_x were emitted during this period among other trace gases [*Pfister et al.*, 2005]. Because CO is a precursor of ozone and has a long residence time, it is known as a good tracer of polluted air masses. Figure 1 shows the MOPITT (Measurement Of Pollution In The Troposphere) [*Drummond and Mand*, 1996; *Deeter et al.*, 2003, 2004] carbon monoxide (CO) retrievals at 500 hPa between 15 July and 15 August 2004, along with the corresponding horizontal wind field from Météo-France ARPEGE [*Courtier et al.*, 1991] meteorological analyses. Maximum CO mixing ratios are localized over Alaska and Canada because of wildfire events during this period. The strong zonal flow above Alaska and the following low-pressure system allowed the rapid transport of CO and other burning by-products toward the contiguous United States and the North Atlantic [*Fuelberg et al.*, 2007]. Previous work has established that biomass burning events strongly impacted atmospheric chemistry from North America to Europe during the summer 2004 [*Cook et al.*, 2007; *Methven et al.*, 2006]. Deep convection and lightning were also found to be important factors [*Singh et al.*, 2007].

[5] Modeling constitutes an essential complement to measurements in order to quantify and understand chemical processes in the atmosphere. Numerous studies have shown the capacity of global chemistry transport models (CTM) to reproduce the main characteristics of atmospheric chemical composition [*Wang et al.*, 1998; *Bey et al.*, 2001; *Horowitz et al.*, 2003]. Models are needed for future projections of atmospheric composition. Model evaluation of extreme

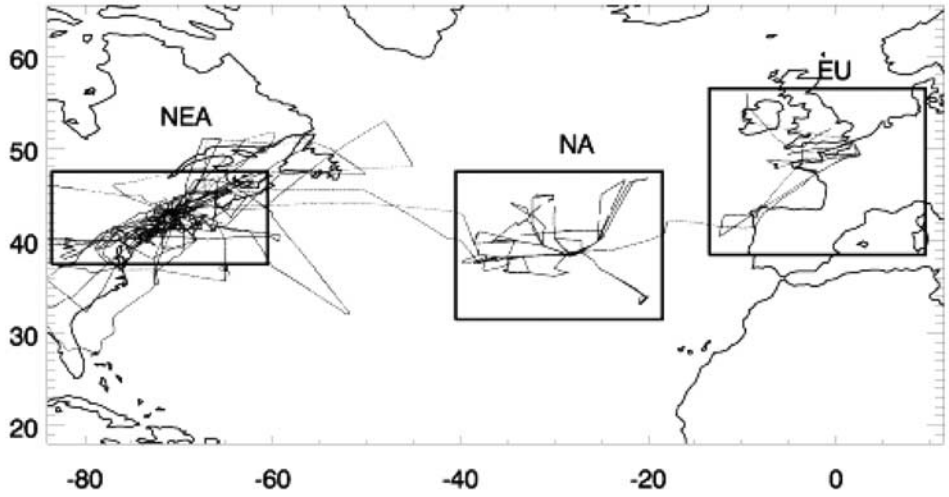

Figure 2. Regions used to aggregate the aircraft observations for the purpose of the model evaluation. The different boxes correspond to (from left to right) northeast America (NEA), North Atlantic (NA), and Europe (EU). Flight trajectories have been superimposed (black lines).

Table 1. MOCAGE Emissions Inventories Used for the ITOP Simulation

Species[a]	Definition	Biomass Burning[b]	Other Sources[b]
CO	carbon monoxide	1	2
NO_x (= NO + NO_2)	nitrogen dioxide and nitric oxide	1	2
TOL	toluene and less reactive aromatics	1	1
CH_4	methane	1	2
HC_5	alkanes, alcohols, esters and alkynes with HO rate constant between 3.4×10^{-12} and 6.8×10^{-12} cm^3 s^{-1}	1	1
ALD	acetaldehyde and higher aldehydes	1	1
HCHO	formaldehyde	1	1
HC_3	alkanes, alcohols, esters and alkynes with HO rate constant less than 3.4×10^{-12} cm^3 s^{-1}	1	1
ETH	ethane	1	1
ETE	ethene	1	1
KET	ketones	1	1
OLI	internal alkenes	1	1
OLT	terminal alkenes	1	1
Others		2	2

[a]See *Stockwell et al.* [1997].
[b]Inventories: 1, daily emissions over the United States from *Pfister et al.* [2005]; 2, monthly or yearly emissions from *Dentener et al.* [2004, 2006].

events and variability, in addition to averages, is crucial for characterizing uncertainties. However, model performance is strongly dependent on horizontal resolution [*Crowther et al.*, 2002; *Jang et al.*, 1995], and current state-of-the-art global models are currently presenting horizontal resolutions of 2° or coarser. For the ITOP campaign in particular, atmospheric dynamics over the North Atlantic midlatitudes, spatial variablity of the continental emissions and other surface processes call for high spatial resolution. In addition, the high variability in space and time of the North American wildfires during the summer 2004 requires a daily biomass burning emission inventory in the model. Here, we assess the capability of the MOCAGE (MOdèle de Chimie Atmosphérique à Grande Echelle, Model of Atmospheric Chemistry at Large Scale) CTM to simulate the general features of the distribution of tropospheric ozone and related species during the ICARTT/ITOP campaign. The simulation was performed using a high-resolution grid (0.5° × 0.5°) over the North Atlantic coupled to a global grid (2° × 2°) providing the time-dependent boundary conditions. A daily inventory of biomass burning emissions for North America [*Pfister et al.*, 2005] was used to take into account the high temporal and spatial variability of the fire events. Results were subsequently compared with aircraft in situ measurements and satellite data (MOPITT CO and SCIAMACHY (Scanning Imaging Absorption Spectrometer for Atmospheric Chartography) NO_2). This evaluation displays the principal characteristics of the MOCAGE model and is intended to provide background for future and ongoing studies using this model.

[6] The structure of the paper is the following. Section 2 presents the model setup. Aircraft and satellite data along with the comparison methods are described in section 3. Results of the MOCAGE simulation are discussed in section 4. We summarize our results and conclude in section 5.

2. Model Setup

[7] The MOCAGE model is a global 3-D CTM providing numerical simulations of the interactions between dynamical, physical and chemical processes in the troposphere and lower stratosphere. MOCAGE uses a semi-Lagrangian advection scheme [*Josse et al.*, 2004] to transport the chemical species. We used two nested domains for our simulation: a global grid with a horizontal resolution of 2° × 2° and a regional grid (Lat: 12–66°N, Lon: 84°W–12°E) with a horizontal resolution of 0.5° × 0.5° (see Figure 2). We use the outputs corresponding to the regional grid for our study. MOCAGE includes 47 hybrid (σ, p) levels from the surface up to 5 hPa. The vertical resolution is 40 to 400 m in the boundary layer (7 levels) and about 800 m in the vicinity of the tropopause and in the lower stratosphere. The chemical scheme used is RACMOBUS, which combines the stratospheric scheme REPROBUS [*Lefèvre et al.*, 1994] and the tropospheric scheme RACM [*Stockwell et al.*, 1997]. RACMOBUS includes 119 individual species, among which 89 are prognostic variables, and considers

Table 2. DC-8 Payload[a]

Parameters	Method	Principal Investigators	Detection Limit/Response (Nominal Accuracy)
O_3	NO/O_3 chemiluminescence	M. Avery, NASA LaRC	1 ppb/1 s (±5%)
CO	TDL absorption spectrometry chemiluminescence	G. Sachse, NASA LaRC	1 ppb/5 s (±5%)
HNO_3, H_2O_2	CIMS	P. Wennberg, Cal Tech	5 ppt/10 s (±15%)
NO_2	LIF and thermal dissociation	R. Cohen, UC Berkeley	1 ppt/60 s (±10%)
ethane, isoprene	whole air samples; GC-FID/EC/MS	D. Blake, UC Berkeley	1 ppt/100 s (±2–10%)
OH	LIF	W. Brune, Penn State Univ.	0.02 ppt/15 s (±15%)
NO chemiluminescence	NO	W. Brune, Penn State Univ.	5 ppt/5 s (±30%)
PAN acetone, mek	GC-ECD/PID/RGD	H. Singh, NASA ARC	1 ppt/90 s (±15%)
HCHO	derivative HPLC and fluorescence	B. Heikes, U. Rhode Island	20 ppt/150 s (±20%)

[a]From *Singh et al.* [2006].

Table 3. BAE-146 Payload[a]

Parameters	Method	Principal Investigators	Detection Limit/Response (Nominal Accuracy)
NO	NO/O_3 chemiluminescence	D. Stewart, Univ. East Anglia	40 ppt/10 s (±10%)
O_3	UV absorption	FAAM[b]	2 ppb/4 s (±5%)
CO	VUV resonance fluorescence	FAAM[b]	2 ppb/1 s
HCHO	Hantzsch fluorometric	G. Mills, Univ. East Anglia	50 ppt/10 s (±30%)
PAN	dual GC/ECD	L. Whalley, Leeds Univ.	10 ppt/90 s (±10%)
Ethane acetone, isoprene	dual channel grab sample/GC	J. R. Hopkins, Univ. York	2 ppb/60 s

[a]From *Fehsenfeld et al.* [2006].
[b]Facility of Airborne Atmospheric Measurements (FAAM), UK.

372 chemical reactions. For the RACM mechanism, the VOCs species in the real atmosphere are aggregated into 16 anthropogenic and 3 biogenic model species, the grouping being based on the magnitudes of the emission rates, similarities in functional groups and the compound's reactivity toward OH. Biogenic emissions of hydrocarbons from vegetation include isoprene, monoterpenes, and other VOC emissions; monthly distributions are taken from *Guenther et al.* [1995], and totals are those of *Dentener et al.* [2004] (e.g., 503 Tg(C)/year for isoprene). Convective processes are simulated with the scheme of *Bechtold et al.* [2001], turbulent diffusion is calculated with the scheme of *Louis* [1979]. A lightning NO_x source (LiNOx) has been implemented in the deep convective scheme following a mass-flux formalism coherent with the transport [*Mari et al.*, 2006]. In this approach, the LiNOx production inside clouds is based on critical levels defined in the deep convective scheme. Once produced inside the convective column, NO molecules are redistributed by updraft and downdraft and detrained in the environment when the conditions are favorable. MOCAGE also parameterizes dry deposition: the deposition velocity of about hundred compounds including ozone, nitrogen-containing compounds, as well as long-lived and short-lived intermediates organic compounds, was parameterized on the basis of *Wesely* [1989], using the ''big-leaf'' resistance approach [*Michou and Peuch*, 2002; *Michou et al.*, 2005; *Nho-Kim et al.*, 2004]. The model distinguishes between convective and stratiform precipitation. Wet deposition of soluble species in convective updraft is based on the mass flux approach described by *Mari et al.* [2000]. The removal in large-scale stratiform precipitation is treated as a first-order process [*Giorgi and Chameides*, 1986]. Rain out below cloud follow *Liu et al.* [2001]. The model uses the emission inventory from *Dentener et al.* [2004] with a monthly or yearly resolution depending on the species. Emissions by aircraft are not included in the model. However, because of the strong intensity and variablity of the North America wildfire events during summer 2004, we used for several species the daily North America emission inventory of *Pfister et al.* [2005]. For more details about the source inventories used in the model see Table 1. The meteorological analyses of Météo-France [*Courtier et al.*, 1991] were used to initialize and constrain the dynamics of the model every 3 hours. The vertical velocity is calculated from the ARPEGE wind horizontal components by imposing the mass conservation law for each atmospheric column. Our simulation started from a climatological initial field on 1 June 2004 at 0000 UT.

3. Rationale of the Evaluation

3.1. Chemical Species

[8] We focused our evaluation of MOCAGE on the following species: OH, H_2O_2, CO, NO, NO_2, PAN, HNO_3, isoprene, ethane, ketones, HCHO and O_3. OH is the main oxidant for nonradical species in the atmosphere. OH concentration is of primary importance for quantifying chemical processes in the troposphere, in particular the formation and destruction of O_3. The radical OH is chiefly formed by O_3 photolysis as follows:

$$O_3 + h\nu \rightarrow O_2 + O(^1D) \quad (1)$$

$$O(^1D) + H_2O \rightarrow 2OH \quad (2)$$

[9] In most of the troposphere, production of H_2O_2 is the principal sink for HO_x (HO_x = H + OH + HO_2) via the reaction:

$$HO_2 + HO_2 \rightarrow H_2O_2 + O_2 \quad (3)$$

[10] H_2O_2 is highly soluble in water and then removed by scavenging on a timescale of a week. Besides its fundamental role in tropospheric chemistry as the main OH source, O_3 is known to be toxic to humans and vegetation because it oxidizes biological tissue [*Vandeirmeiren et al.*, 2005]. In the troposphere, O_3 production consists of oxidation reactions between OH and some trace gas constituents in the presence of NO_x. One of the precursors of O_3 is CO, which is produced by incomplete combustion of hydro-

Table 4. FALCON-DLR Payload[a]

Parameters	Method	Principal Investigators	Detection Limit/Response (Nominal Accuracy)
CO	VUV resonance fluorescence	H. Schlager, Institut for Atmospheric Physics	1 ppb/1 s (±5%)
NO	NO/O_3 chemiluminescence	H. Schlager, Institut for Atmospheric Physics	2 ppt/1 s (±7%)
O_3	UV Absorption	H. Schlager, Institut for Atmospheric Physics	0.5 ppb/5 s (±5%)

[a]From *Fehsenfeld et al.* [2006].

Table 5. MOZAIC Payload[a]

Parameters	Method	Principal Investigators	Detection Limit/Response (Nominal Accuracy)
CO	IR GFC	P. Nédélec, Laboratoire d'Aérologie	5 ppb/30 s (±5%)
O_3	UV absorption	A. Marenco, Laboratoire d'Aérologie	2 ppb/4 s (±2%)

[a]From *Nédélec et al.* [2003] and *Marenco et al.* [1998].

carbons and plays a key role in tropospheric chemistry. The average lifetime of CO at midlatitudes is about one month. Hydrocarbons oxidation is of primary importance in the regulation of tropospheric OH and O_3 concentrations. Ethane is released by industrial and combustion sources and is removed by OH oxidation with a lifetime of a few months. HCHO is a by-product of hydrocarbons oxidation and is mainly produced by methane and VOCs. It can be scavenged by clouds but its lifetime is long enough to allow transport in remote regions where its photolysis produces HO_x radicals. The principal biogenic hydrocarbon contributing to O_3 formation is isoprene, an odorless compound that is a by-product of photosynthesis. Isoprene reacts extremely rapidly with OH, resulting in an atmospheric lifetime of less than one hour. NO_x are produced by combustion processes, lightning and soil decomposition. NO_x concentrations control to a large part O_3 production and destruction in the troposphere and thus play a key role in air quality. An important sink of NO_x is its oxidation to HNO_3 which is highly soluble in water and can be scavenged by precipitation in the troposphere. PAN is produced in the troposphere by photochemical oxidation of carbonyl compounds in the presence of NO_x. The lifetime of PAN strongly depends on temperature, varying from 1 hour at 295 K to several months at 250 K. In the lower troposphere, NO_x and PAN are near chemical equilibrium. However, in the middle and upper troposphere, PAN is a reservoir for NO_x. It can be transported over long distances and decomposed to release NO_x far from its source. Ketones originate from direct emissions of biogenic and anthropogenic sources and are by-products of NMHCs oxidation. These species are important precursors of PAN.

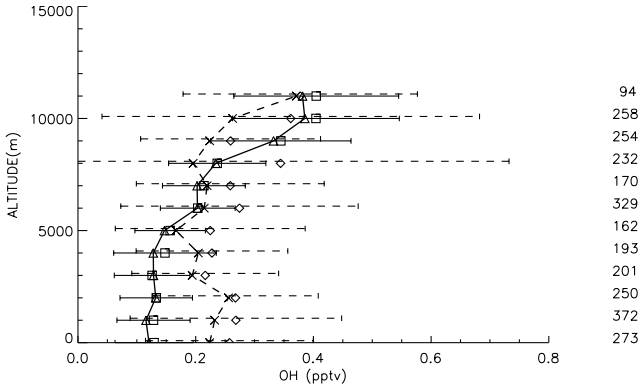

Figure 3. Comparison of observed and simulated vertical profile of OH (pptv) over the NEA domain (DC8 flights). The open squares are mean observed values (with horizontal bars for the standard deviation), and the open triangles and solid lines are median observed values. Open diamonds are mean simulated values, and cross and dotted lines are median simulated values (with horizontal bars for standard deviations); values on the right are the number of data averaged for each level.

3.2. Data

[11] The in situ measurements considered in this study were made aboard several mobile platforms: the aircraft FAAM BAE 146 from the Institute for Atmospheric Science (UK), DC-8 from the NASA Project Office (USA), Falcon from the Institute of Atmospheric Physics (Germany) and MOZAIC (Measurement of Ozone and water vapor by Airbus in-service Aircraft) [*Nédélec et al.*, 2003; *Thouret et al.*, 1998]. We further used data from the remote sensing instruments MOPITT and SCIAMACHY.

[12] Specifications for aircraft in situ measurements are summarized in Tables 2–5. The method used to compare in situ measurements with the model is the following: We first averaged all the data sets over 1-min intervals. Then, for each data point, an online interpolation in time and space was performed to derive the corresponding model value. The observed and simulated data were finally averaged to obtain mixing ratio profiles with 1 km vertical resolution over three regions for the whole duration of the campaign: northeastern America (NEA), North Atlantic (NA) and Europe (EU). Figure 2 presents the 3 domains mentioned above superimposed with all the ITOP flight tracks. For the NEA domain, we used data from the MOZAIC and DC-8 platforms. For the NA domain, we used measurements from the BAE-146 platform. Finally, for the EU domain, we used data from MOZAIC and the Falcon-DLR. Note that all chemical species are not always available over the three domains.

[13] MOPITT is a nadir infrared correlation radiometer onboard the NASA Terra Satellite [*Drummond and Mand*, 1996]. It has a horizontal resolution of 22 km × 22 km and provides global coverage in about 3 days. We used the

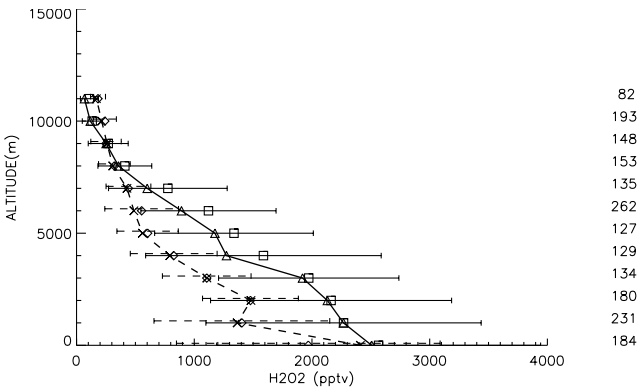

Figure 4. Same as Figure 3 but for H_2O_2 (pptv).

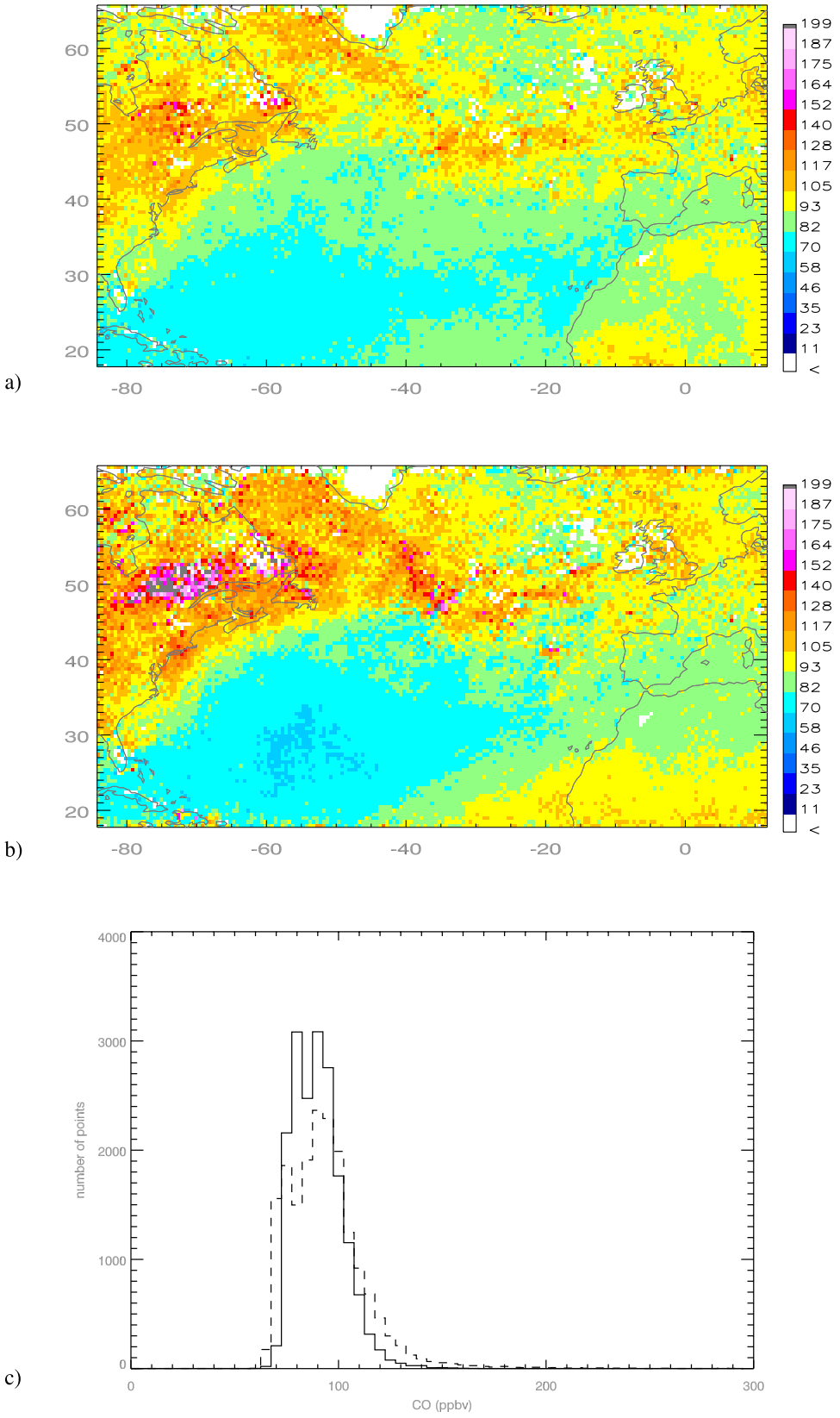

Figure 5. Comparison between MOPITT and MOCAGE CO (ppbv) during ITOP at 500 hPa. (a) MOPITT CO binned at 0.5° × 0.5°, (b) MOCAGE CO binned at 0.5° × 0.5°, and (c) corresponding histograms of MOCAGE (dashed line) and MOPITT CO (solid line).

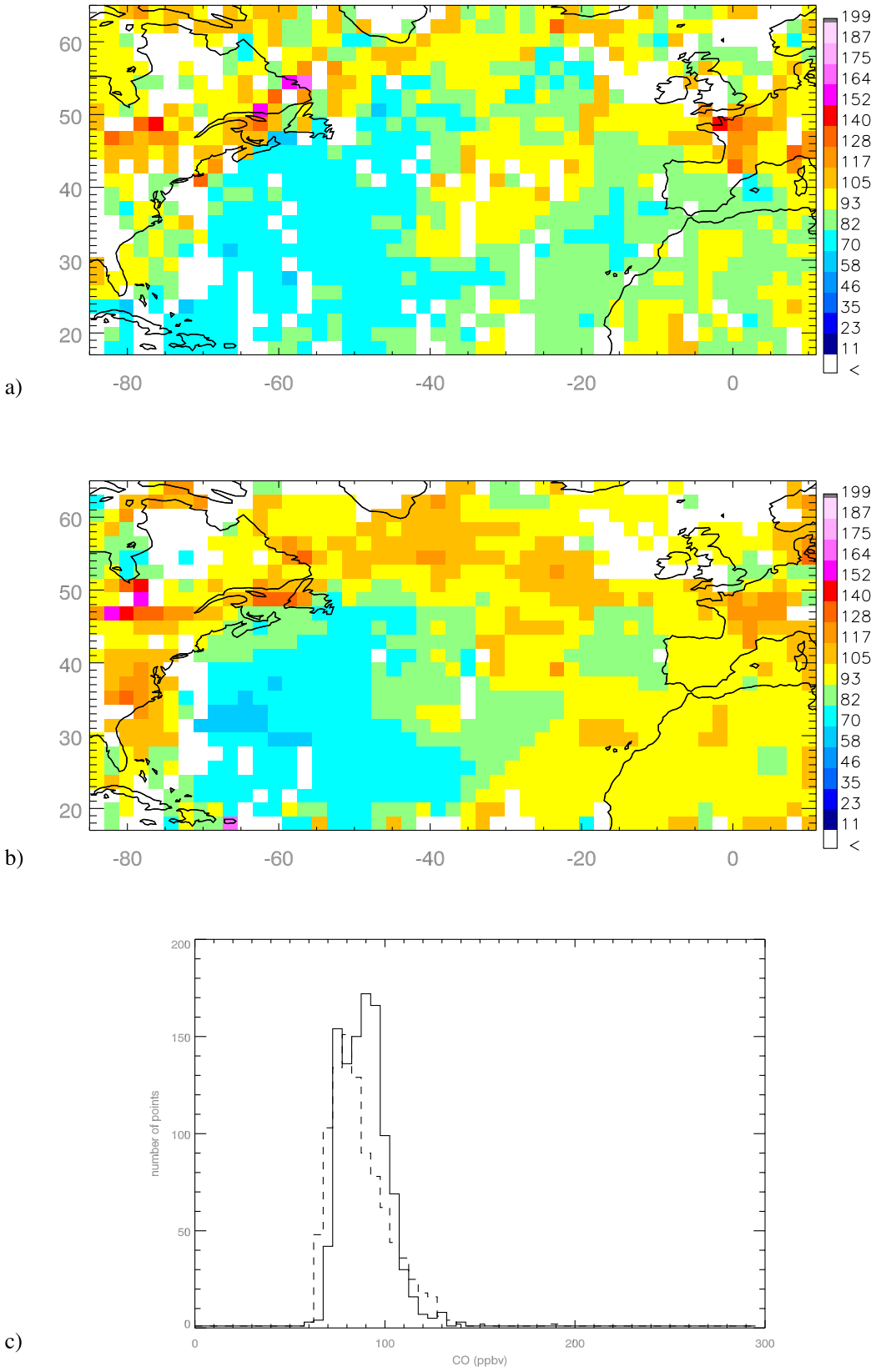

Figure 6. Comparison between (a) MOPITT CO (ppbv) binned at 2° × 2° and (b) MOCAGE CO (ppbv) for the 2° × 2° simulation at 500 hPa between 24 and 26 July 2004 and (c) corresponding histograms of MOCAGE (dashed line) and MOPITT CO (solid).

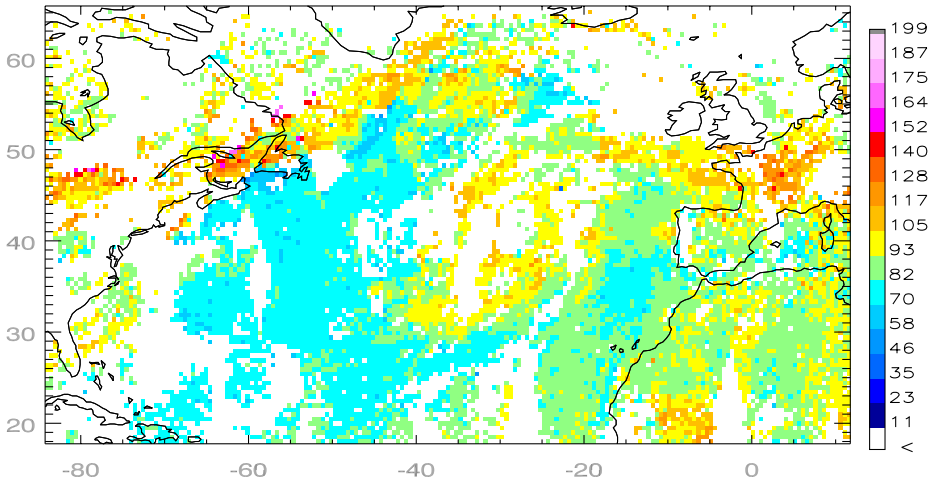

a)

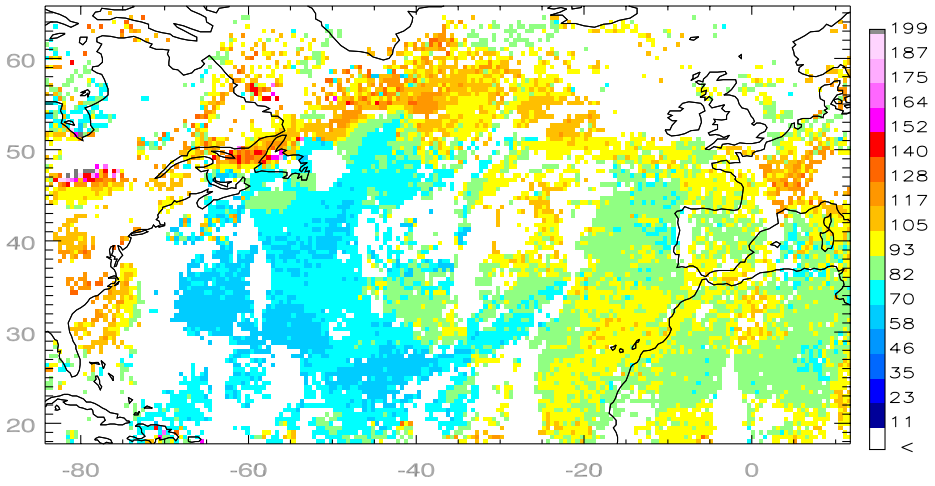

b)

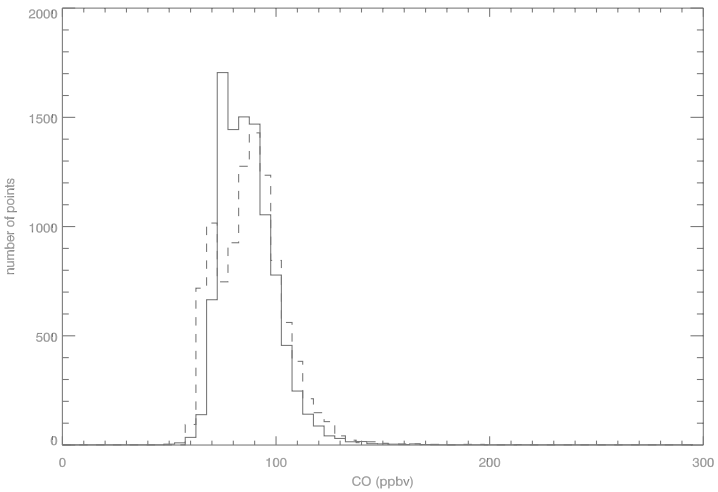

c)

Figure 7. Comparison between (a) MOPITT CO (ppbv) binned at 0.5° × 0.5° and (b) MOCAGE CO (ppbv) for the 0.5° × 0.5° simulation at 500 hPa between 24 and 26 July 2004 and (c) corresponding histograms of MOCAGE (dashed line) and MOPITT CO (solid).

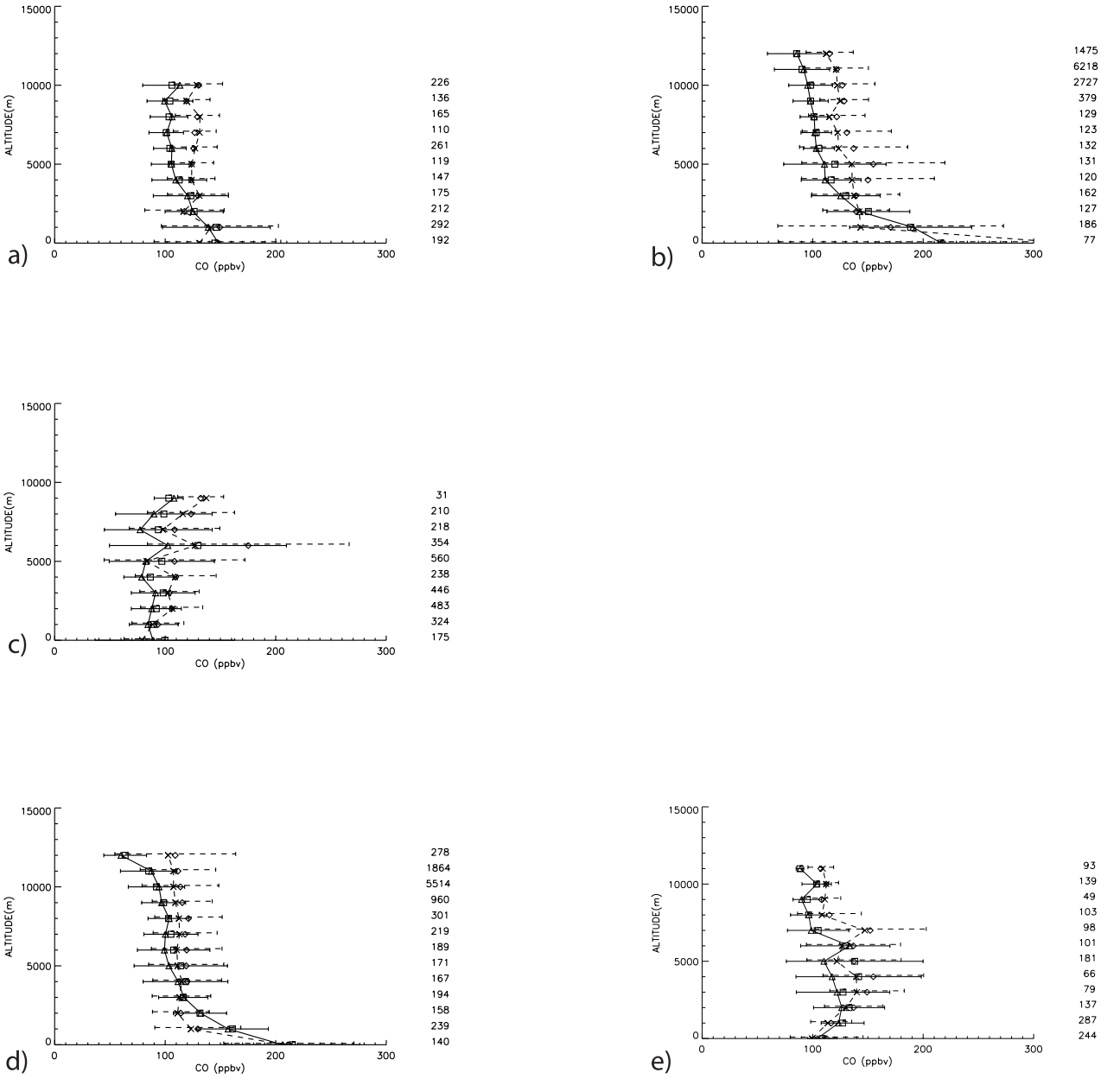

Figure 8. Same as Figure 3 but for CO (ppbv): (a) DC8, NEA domain; (b) MOZAIC, NEA domain; (c) BAE-146, NA domain; (d) MOZAIC, EU domain; and (e) FALCON, EU domain.

Level 2 V3 MOPITT data sets, which consist of retrieved CO mixing ratios for 7 vertical levels in the atmosphere (surface, 850 hPa, 700 hPa, 500 hPa, 350 hPa, 250 hPa and 150 hPa). A detailed description of the MOPITT-CO retrievals is given by *Deeter et al.* [2003].

[14] SCIAMACHY observes the upwelling radiation from the earth surface and the extraterrestrial solar radiance. It alternately measures in nadir and limb, covering the 220–2240 nm spectral region range with a resolution of 0.25 nm in the UV, 0.4 nm in the visible and less than 0.4 nm in the Near Infra Red (NIR). Here we used the NO_2 tropospheric column product. The typical size of the nadir ground-pixel for NO_2 is 30 km $\times$ 60 km. Its swath width is 960 km, providing global coverage at the equator within 6 days. The retrieval approach used for NO_2 nadir measurements is based on the Differential Optical Absorption Spectroscopy (DOAS) method. Details on the data analysis are given by *Richter and Burrows* [2002].

[15] To compare MOCAGE with MOPITT retrievals, we performed for each data point a time-space interpolation online in the model within each time step and transformed the MOCAGE CO profiles using the corresponding averaging kernels [*Emmons et al.*, 2004]. The MOCAGE tropospheric column of NO_2 was calculated by integrating the column from the surface to the tropopause. We consider the height of the tropopause as the minimum altitude between the level with potential vorticity equal to 2 PVU and the level with potential temperature equal to 380 K. This method has little impact on the model agreement with the satellite data [*Savage et al.*, 2004] and avoids the

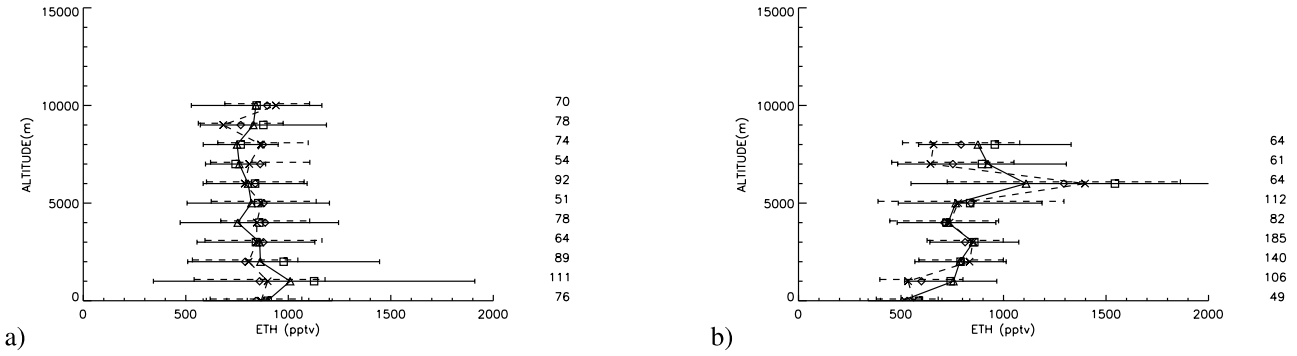

Figure 9. Same as Figure 3 but for ethane (pptv): (a) DC8, NEA domain, and (b) BAE-146, NA domain.

problem of bias linked to the uncertainty in modeled stratospheric NO_2 encountered in the reference sector method [*Richter and Burrows*, 2002]. MOCAGE NO_2 columns were interpolated in space and time to the SCIAMACHY pixels off-line using the outputs at 0000, 0600, 1200 and 1800 UTC.

4. Results and Discussions

4.1. Hydroxyl Radical and Hydrogen Peroxide

[16] Figures 3 and 4 present the profiles of OH and H_2O_2, respectively, for the NEA domain.

[17] Modeled OH is about 2 times the observed OH between 0 and 4 km. There is better agreement above 5 km, but with an underestimation of about 30% between 9 and 10 km. In the lower troposphere, Volatile Organic Compounds (VOC), such as isoprene and ethane, have a strong influence on OH mixing ratio [*Di Carlo et al.*, 2004]. There is no significant bias in the model for this species (see Figures 9 and 11). X. Ren et al. (HOx observation and model comparison during INTEX-NA 2004, submitted to *Journal of Geophysical Research*, 2006) have shown that during the INTEX-NA experiment, observed OH and HO_2 mixing ratios were lower than expected from box model and CTM calculations (MOZART, RAQMS, GEOS-CHEM) over most of the troposphere. They found that, on average, OH was overpredicted by a factor of 1.7 and suggested the presence of unknown atmospheric constituents or unknown reactions that remove OH. A similar conclusion was made by *Di Carlo et al.* [2004], who studied OH reactivity in a northern Michigan forest. Another factor which could explain part of our bias in the lower troposphere is that MOCAGE does not include photochemical effects of aerosols: aerosol scattering, absorption of ultraviolet radiation and reactive uptake of HO_2, NO_2 and NO_3. Indeed, *Martin et al.* [2003] have investigated these effects on tropospheric oxidants and found that aerosols uptake of HO_2 accounts for 10–40% of total HO_x radical loss in the boundary layer over polluted continental regions.

[18] H_2O_2 mixing ratio decreases with altitude both in the measurements and in the model because of the air masses drying. Simulated H_2O_2 mixing ratios are lower than observations between 0 and 7 km, with a mean underestimation of about 28%. These discrepancies suggest that the HO_x loss reaction (3) might be too low in our model, which is consistent with an overestimation of OH along with an underestimation of H_2O_2.

4.2. Carbon Monoxide

[19] Figure 5 shows the comparisons between MOCAGE and MOPITT CO at 500 hPa for the period 15 July to 15 August 2004. The model reproduces well the observed distribution. The pathway of exported pollution is centered around 50°N. Both in the observations and in the simulation, maximum CO values are found over eastern Canada because of the transport of biomass burning plumes in this area and the persistence of a convergence zone (see Figure 1). The correlation coefficient (r^2) between the model and the observations at this level is approximately 0.98. The histograms shown in Figure 5c. are very similar but the model has a larger range of values than the observations. In order to investigate the impact of the

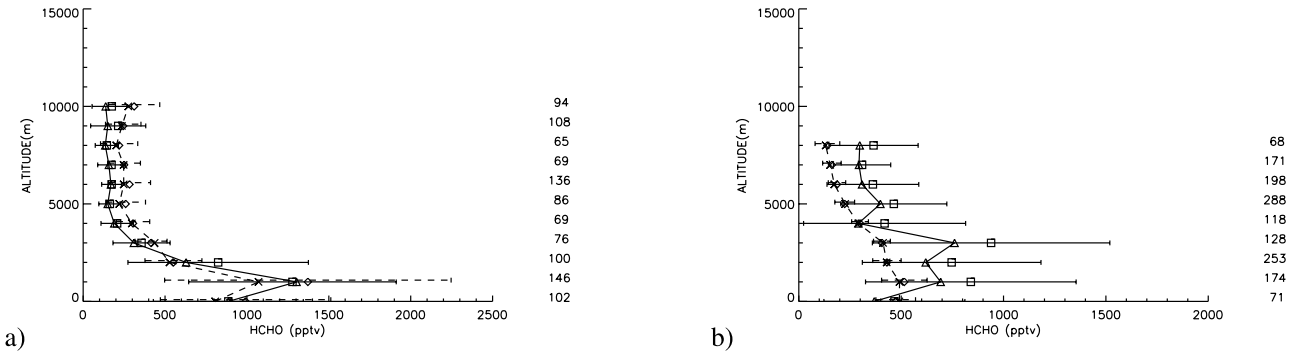

Figure 10. Same as Figure 3 but for HCHO (pptv): (a) DC8, NEA domain, and (b) BAE-146, NA domain.

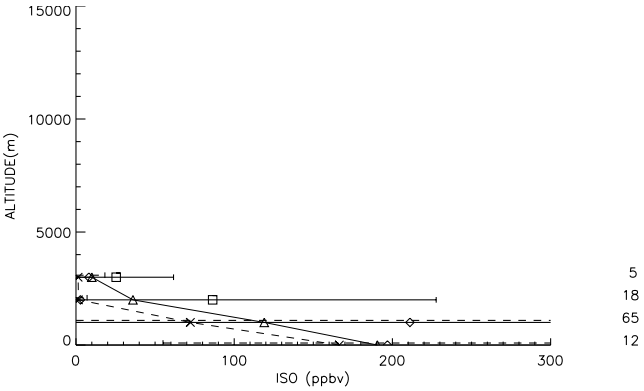

Figure 11. Same as Figure 3 but for isoprene (ppbv) over the NEA domain (DC8).

resolution, we performed two model simulations between 24 and 26 July 2004 at $2° \times 2°$ and $0.5° \times 0.5°$ resolution respectively, and compared the results with MOPITT data. Figure 6 shows MOCAGE $2° \times 2°$ simulation and MOPITT CO at 500 hPa binned at $2° \times 2°$ while Figure 7 shows model and observations binned at $0.5° \times 0.5°$. We clearly see a synoptic-scale structure over the Atlantic in the central part of the domain on the MOPITT measurements which is better reproduced in the $0.5° \times 0.5°$ simulation than in the $2° \times 2°$ simulation. The corresponding histograms confirm there is a better agreement with MOPITT data using high-resolution grid instead of low-resolution grid, with a figure of merit (fom) of 0.70 and 0.65 respectively.

[20] Figure 8 displays the measured and simulated vertical profiles of CO. Over the NEA domain, (Figures 8a and 8b) the shapes of the profiles are well reproduced, both for the MOZAIC and the DC8 observations. Maximum mixing ratios are found in the lower troposphere where there is a significant influence of anthropogenic emissions. The lower troposphere concentrations as well as the gradient are higher in the MOZAIC profiles because MOZAIC measurements of the lower troposphere occur over urban areas while the DC8 aircraft missions sampled also the marine boundary layer. There is an overestimation of about 20–30 ppbv over the NEA domain above 3 km of altitude. Given the consistency between CO estimations from *Turquety et al.* [2007] and *Pfister et al.* [2005], the CO emissions used can be considered as quite realistic and are not to blame. A high amount of hydrocarbon species like CH_2O were released by North American wildfires during ITOP/ICARTT period. As we discussed above, OH mixing ratios are too high in the lower troposphere in the model. Thus the CO overestimation over the NEA domain might result from a higher hydrocarbons oxidation by OH near the fire sources. The shape of the CO profile is well reproduced by the model over the NA domain. In particular there is a peak at 6 km both in the model and in the measurements, which corresponds to the altitude where plumes were transported across the Atlantic [*Cook et al.*, 2007]. There are high standard deviations both in the measurements and in the model around 6 km altitude that reflect the high variability of the LRT events. The 20 ppbv bias evident throughout the troposphere lies within the variability of the observations. Over the EU domain, the modeled profile is consistent with the MOZAIC measurements. This profile is very similar to the MOZAIC profile over the NEA domain. The Falcon profile is well reproduced by the model but with a shift of 1 km for the observed peak at 6 km. This peak has to be linked with the same peak over the NA domain as the Falcon aircraft missions were designed to intercept biomass burning plumes and anthropogenic plumes coming from North America.

4.3. Hydrocarbons and Ketones

[21] Comparisons for ethane are shown in Figure 9. For the NEA domain, there is a good agreement between the model and the observations. The high inhomogeneity of ethane emissions cannot be correctly resolved by the model resolution, which explains the higher variability in the observed values. For the NA domain, the simulated ethane profile is consistent with the observations. In particular, the peak at 6 km linked to LRT events is well captured by the model.

[22] The HCHO comparisons over the NEA domain are presented in Figure 10. Measurements and simulation are in good agreement throughout the troposphere. Observed and simulated concentrations both peak at 1 km, reflecting combined effects of anthropogenic emissions and deposition processes near the ground. Over the NA domain, the model underestimates the observed concentrations by about 55% throughout the troposphere. The corresponding mean negative bias is about 0.16 ppbv, which is consistent with the median measured-modeled [HCHO] difference of 0.13–0.18 ppbv given by *Frost et al.* [2002]. A possible

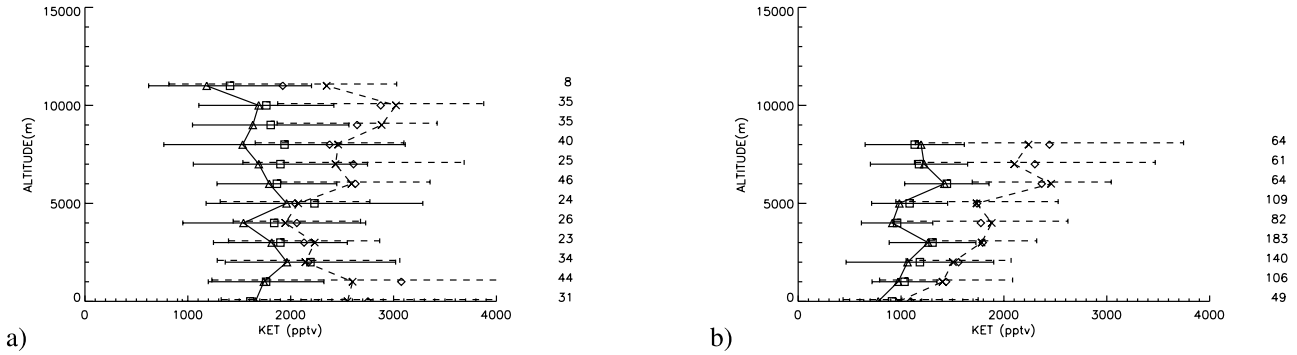

Figure 12. Same as Figure 3 but for ketones (pptv): (a) DC8, NEA domain, and (b) BAE-146, NA domain.

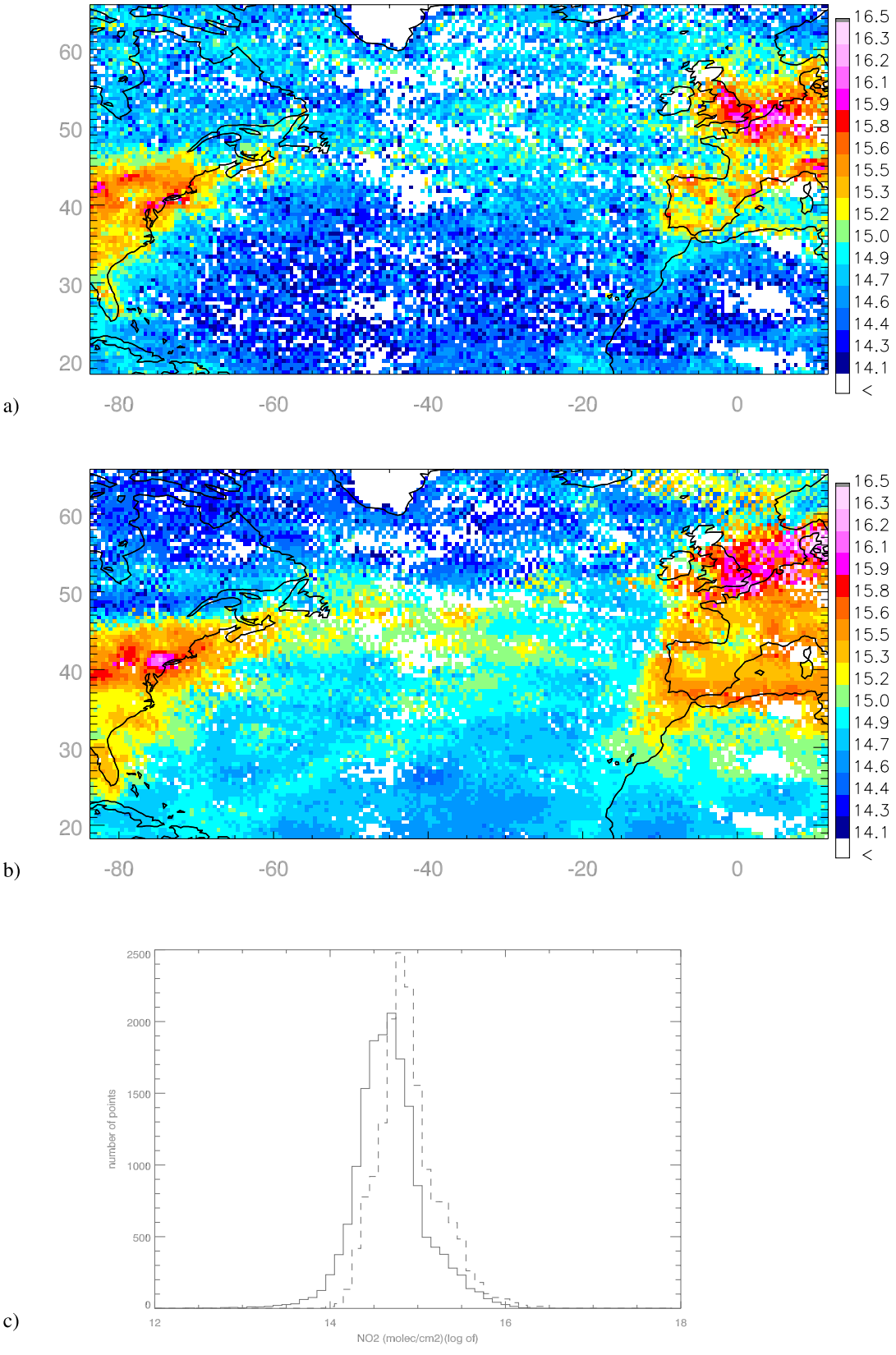

Figure 13. Comparison between SCIAMACHY and MOCAGE NO_2 for the period between 15 July and 15 August 2004. The color code represents the logarithm of the NO_2 (molecules cm^{-2}). (a) NO_2 tropospheric columns from SCIAMACHY, (b) NO_2 tropospheric columns from MOCAGE, and (c) corresponding histograms of MOCAGE NO_2 (dashed line) and SCIAMACHY NO_2 (solid line).

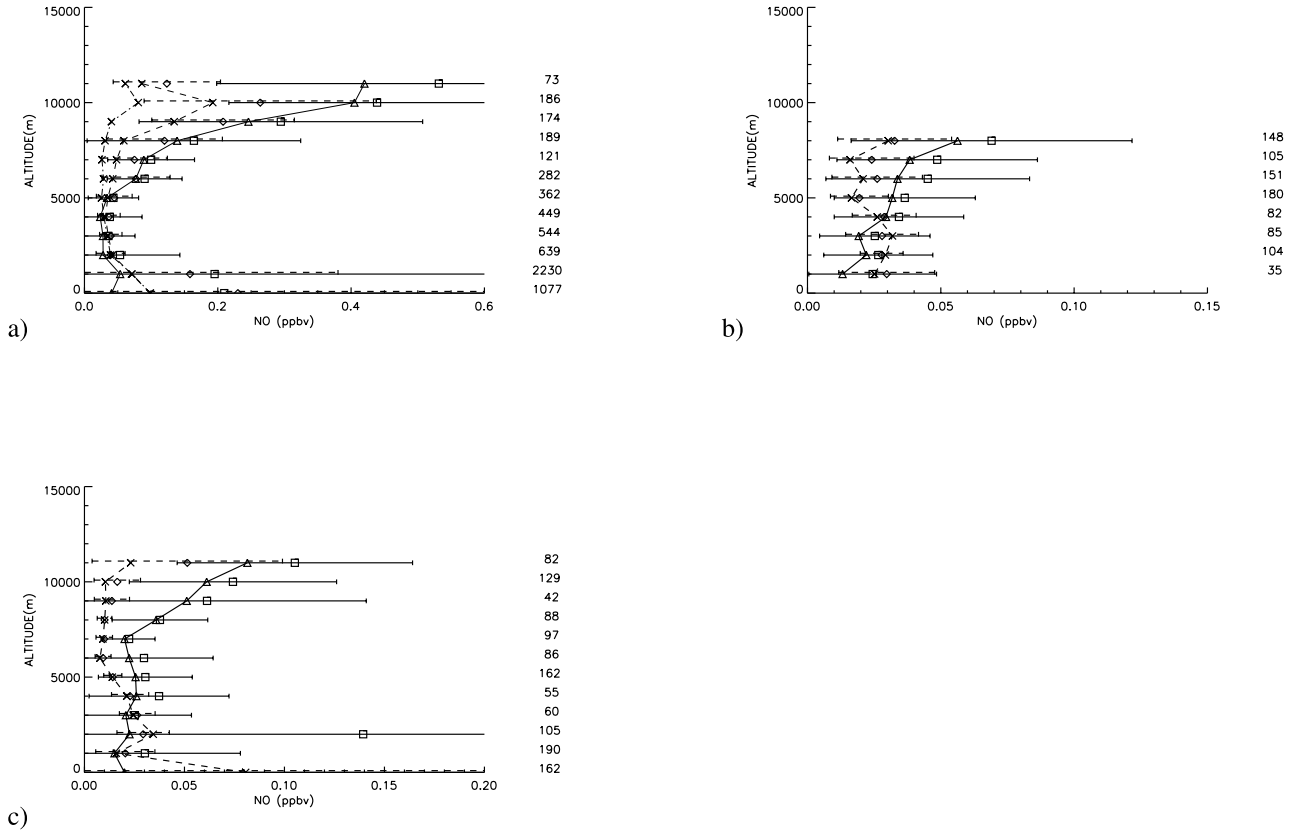

Figure 14. Same as Figure 3 but for NO (pptv): (a) DC8, NEA domain; (b) BAE-146, NA domain; and (c) FALCON, EU domain. For the NEA domain, the dash-dotted line represents the simulation without LiNOx.

explanation suggested by this study was that there are probably some unknown sources of HCHO in the North Atlantic troposphere.

[23] Figure 11 presents the results for isoprene over the NEA domain. Modeled mixing ratios are in quite good agreement with the observations. Highest concentrations are found near the ground because of the emission sources and then decrease rapidly with altitude because of the very short lifetime of isoprene.

[24] Ketones profiles over the NEA and NA domains are displayed in Figure 12. Over the NA domain, the model overestimates ketones mixing ratios throughout the troposphere. The overestimation (about 87%) is most pronounced at altitudes above 3 km, where the atmospheric composition is impacted by the transport of biomass burning products. This overestimation is probably due to a too high oxidation of NMHCs over fires area as suggested previously (see section 4.2). The same remark can be applied to the profiles over the NEA domain where the overestimation above 5 km is about 98%. The model overestimation near the ground (50%) suggests an excess of ketones sources in the model.

4.4. Nitrogen Species

[25] Figure 13 compares the NO_2 tropospheric column retrieved from SCIAMACHY and that simulated by MOCAGE between 15 July and 15 August 2004. MOCAGE has a mean positive bias of about 4 10^{14} molecules cm^{-2} compared with SCIAMACHY data. This discrepancy (≈56%) lies within the uncertainty of the SCIAMACHY retrievals [*Richter and Burrows*, 2002]. The histograms in Figure 13 show that the bias is mostly localized over low and medium concentrations regions, such as the North Atlantic. The correlation coefficient (r^2) between the measurements and the model simulation is about 0.34. As seen from Figure 13, the simulations show a stronger pollution export over the Atlantic than the measurements. Some HNO_3 comparisons between MOCAGE and DC8 measurements in the marine low troposphere (not shown here) suggest a too

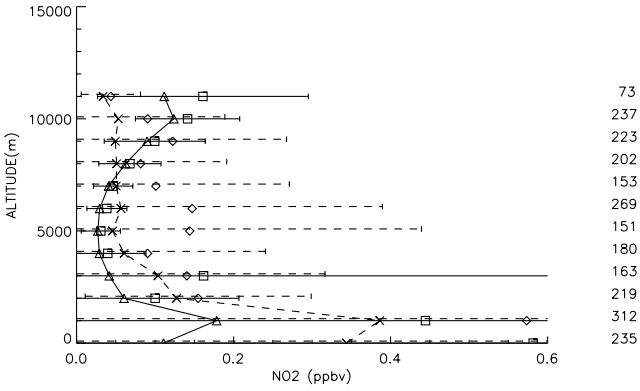

Figure 15. Same as Figure 3 but for NO_2 (pptv) over the NEA domain (DC8).

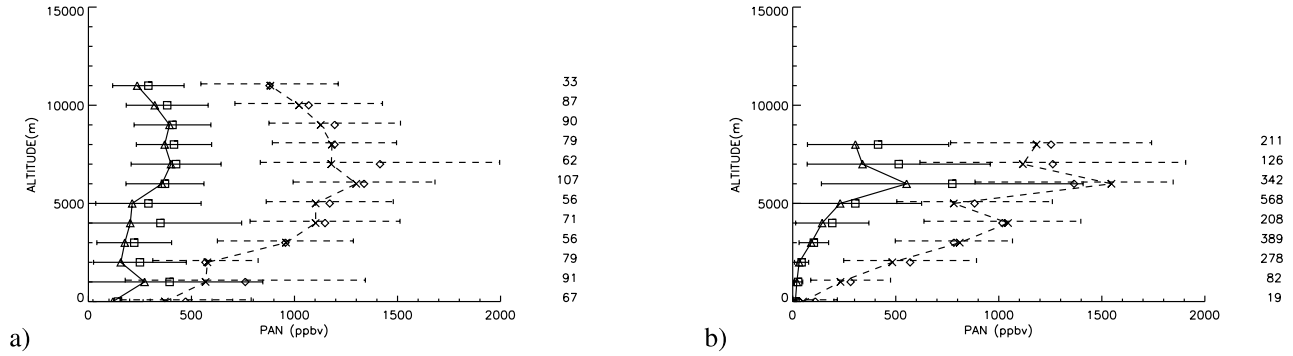

Figure 16. Same as Figure 3 but for PAN (pptv): (a) DC8, NEA domain, and (b) BAE-146, NA domain.

low scavenging in our model in these areas. In addition the NO_2 overestimation might result from too high PAN concentrations in the model (see below), which released NO_2 by thermal decomposition during the transport.

[26] Simulated and observed NO profiles are shown in Figure 14. Over the NEA domain, measurements show a high increase of the NO mixing ratio with altitude between 5 and 11 km typical of lightning activity [*Decaria et al.*, 2005; *Barthe et al.*, 2007; *Höller et al.*, 1999; *Huntrieser et al.*, 1998]. Simulations were performed with and without lightning NO_x (LiNOx) emissions (see Figure 14). Without LiNOx emissions, the model shows no NO enhancement in the upper troposphere. With LiNOx sources however, MOCAGE reproduces the NO peak in the upper troposphere but underestimates its magnitude (by about 200 pptv at 10 km) as it is the case for other CTM (MOZART, GEOS-CHEM, RAQMS) for this period [*Singh et al.*, 2007]. The decrease simulated by the model between 10 and 11 km probably results from a too low cloud height in our convection scheme. These results suggest that lightning contributed significantly to the NO_x budget in the upper troposphere of the United States during the INTEX-NA experiment, as previously reported by *Singh et al.* [2007]. The modeled NO values are consistent with the measurements over the NA domain where there are very low concentrations. Over the EU domain, there is a good agreement between the observations and the simulation at altitudes above 1 km despite a slight underestimation of about 50 pptv in the upper troposphere, probably due to too low lightning NO_x production in the model. The overestimation seen near the ground stays within the range of the observations.

[27] Figure 15 shows the simulated and observed NO_2 profiles over the NEA domain. The shape of the measured profile is well reproduced by the model with the highest values in the lower troposphere and a fast decrease with altitude. The underestimation of NO_2 in the upper troposphere is much less pronounced than for NO and is again due to insufficient lightning sources in the model. There is a significant overestimation of about 116% below 1 km which suggests a too high NOx anthropogenic source over the NEA domain in our inventory.

[28] PAN profiles for the NEA and NA domains are shown in Figure 16. The model systematically overestimates observed mixing ratios, most often by 500–1000 pptv. Significant overestimation of PAN has been shown in the MOZART model [*Horowitz et al.*, 2003], where it was attributed to convective transport of PAN precursors, and lightning sources. As discussed in section 3.1, ketones are produced by hydrocarbons oxidation and are precursors of PAN. The ketones overestimation most likely due to excess of OH in the model (see section 4.3) is thus consistent with the positive bias of PAN.

[29] HNO_3 profile over the NEA domain is shown in Figure 17. The observed mixing ratios are well reproduced between 2 and 8 km altitude. There is an overestimation of about 100% near the ground probably linked to the NO_2 bias previously discussed, as HNO_3 is basically produced by oxidation of NO_2. The slight underestimation in the upper troposphere is again consistent with the NO_2 bias.

[30] Figure 18 presents the NO_y (NO_y = NO + NO_2 + PAN + HNO_3) partitioning over the NEA domain for the model and the observations. NO_y is emitted primarily as NO and is subsequently oxidized in NO_2 and other reactive nitrogen compounds. Thus NO_y partitioning is useful to elucidate the photochemical environment of the air masses [*Neuman et al.*, 2006]. Both in the model and in the measurements, HNO_3 dominates in the lower troposphere and the contribution of PAN increases with altitude up to 8 km, as previously reported by *Singh et al.* [2007]. However, the relative part of PAN in the total reactive nitrogen is overestimated in the model for most of the troposphere. In addition, the contribution of NO_x and HNO_3 in the upper troposphere is much higher for the

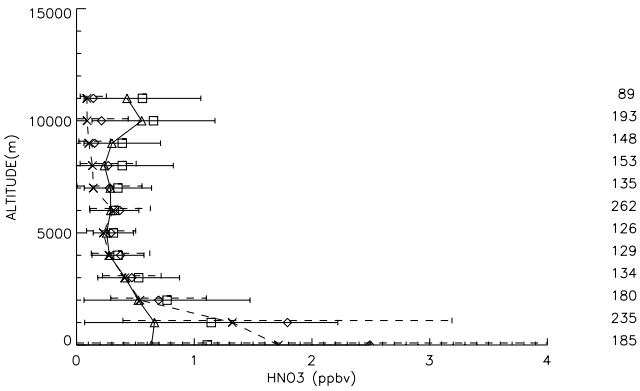

Figure 17. Same as Figure 3 but for HNO_3 (pptv) over the NEA domain (DC8).

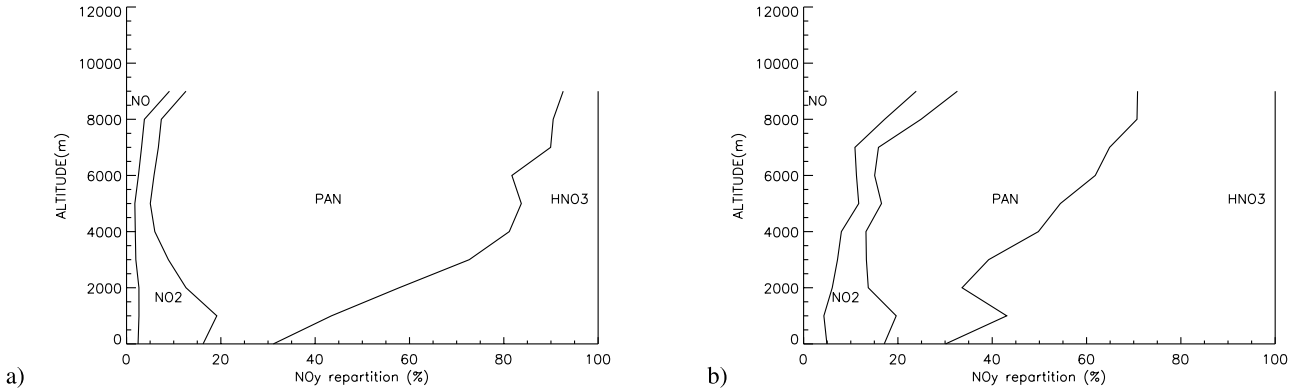

Figure 18. Partitioning of the different species for NO_y (%) (a) for the MOCAGE model and (b) for the DC8 aircraft measurements over the NEA domain.

observations. These discrepancies are due to the underestimation of the NO lightning sources and to the overestimation of PAN concentrations in MOCAGE.

4.5. Ozone

[31] Figure 19 displays O_3 profiles from MOCAGE and from aircraft measurements. Over the NEA domain, for the DC8 profile, there is a mean positive bias of about 12 ppbv for altitudes above 1 km and a surface bias of about 27 ppbv. Similar overestimation was found by the regional air quality model STEM during the ICARTT experiment [*Mena-Carrasco et al.*, 2007]. The study suggested that the ozone bias was due to an overestimation of NO_x emissions. It appears that there is also an excess of NO_x emissions in our model over the NEA domain (see section 4.4). A relatively robust linear relationship exists between NO_y and O_3 in the troposphere as several studies show [*Heland et al.*, 2003]. For instance, a O_3/NO_y ratio of about 10 has been reported near the surface in photochemically aged rural air masses. Assuming this value near the surface over the NEA domain, the MOCAGE NO_y bias could explain 16 ppbv of the corresponding O_3 overestimation. In addition, *Fiore et al.* [2005] have recently investigated the sensitivity of O_3 to uncertainty in isoprene emissions over the United States. Their study shows that the simulated surface O_3 concentrations over the eastern United States can differ up to 15 ppbv when different inventories are used.

[32] For the MOZAIC profiles we have a positive bias in the lower troposphere which reaches 50 ppbv near the surface. Note that the MOZAIC profiles always correspond to a landing or takeoff over airports. This surface bias is higher compared to the one seen for the DC-8 measurements and might be due to an underestimation of NO titration in the model over these highly polluted areas [*Law et al.*, 2000]. In the mid and upper troposphere, the model is in quite good agreement with the measurements. However, the high variability observed in the upper troposphere is not captured in our simulation. The shape of the ozone profiles over the EU and NA domains are well reproduced by the model. We have an overestimation of about 10–20 ppbv throughout the troposphere probably linked to the global excess of oxidation in the model (see previous sections). The peak at 6 km over the NA domain, which corresponds to the LRT events altitude range, is present both in the measurements and in the model and suggests a photochemical production of O_3 during the transport of plumes.

5. Conclusion

[33] In this study, we evaluate the MOCAGE chemistry transport model during the ICARTT/ITOP campaign using several satellite data and aircraft in situ measurements of ozone and precursors. CO comparisons with MOPITT data show that we significantly improve the model results using a higher resolution 0.5° nested domain over the Atlantic, while 2° is the resolution over the rest of the world. The simulated vertical transport appears realistic as the model reproduces well the transport of the plumes over the Atlantic at an altitude of about 6 km. Comparisons with SCIAMACHY retrievals show an excess of tropospheric NO_2 over the North Atlantic in the model which appears to be due to an underestimation of scavenging processes over this area. For most species, the model is capable of representing the general features of the vertical profiles both over continental regions and remote marine environments. However, it appears that too much oxidation occurs in the lower troposphere because of an excess of OH concentrations by a factor of 2. This overestimation results in a global overestimation up to a factor of 2 of some by-products of hydrocarbons oxidation such as PAN and ketones. The variation of NO_y partitioning with altitude over the continental United States is consistent with the observations. However, there is a significant overestimation of PAN contribution throughout the troposphere. NO measurements and a sensitivity test with and without lightning sources of NO_x show a large impact of these sources in the upper troposphere of the northeast United States. As for other global models (GEOS-CHEM, MOZART, RAQMS), this lightning NO source is underestimated in MOCAGE during the summer 2004. The shape of the ozone profiles are well reproduced over the continental Europe and the North Atlantic but there is a global bias of 10–20 ppbv; in the lower troposphere of the northeast United States, the model overestimates the ozone mixing ratio by 30–50 ppbv. This ozone excess is in part due to an overestimation of the lower troposphere NO_y concentrations over these areas and is also probably a consequence of a too high oxidizing environment in the model. Further investigations to characterize the impact of VOCs emissions on OH concentrations

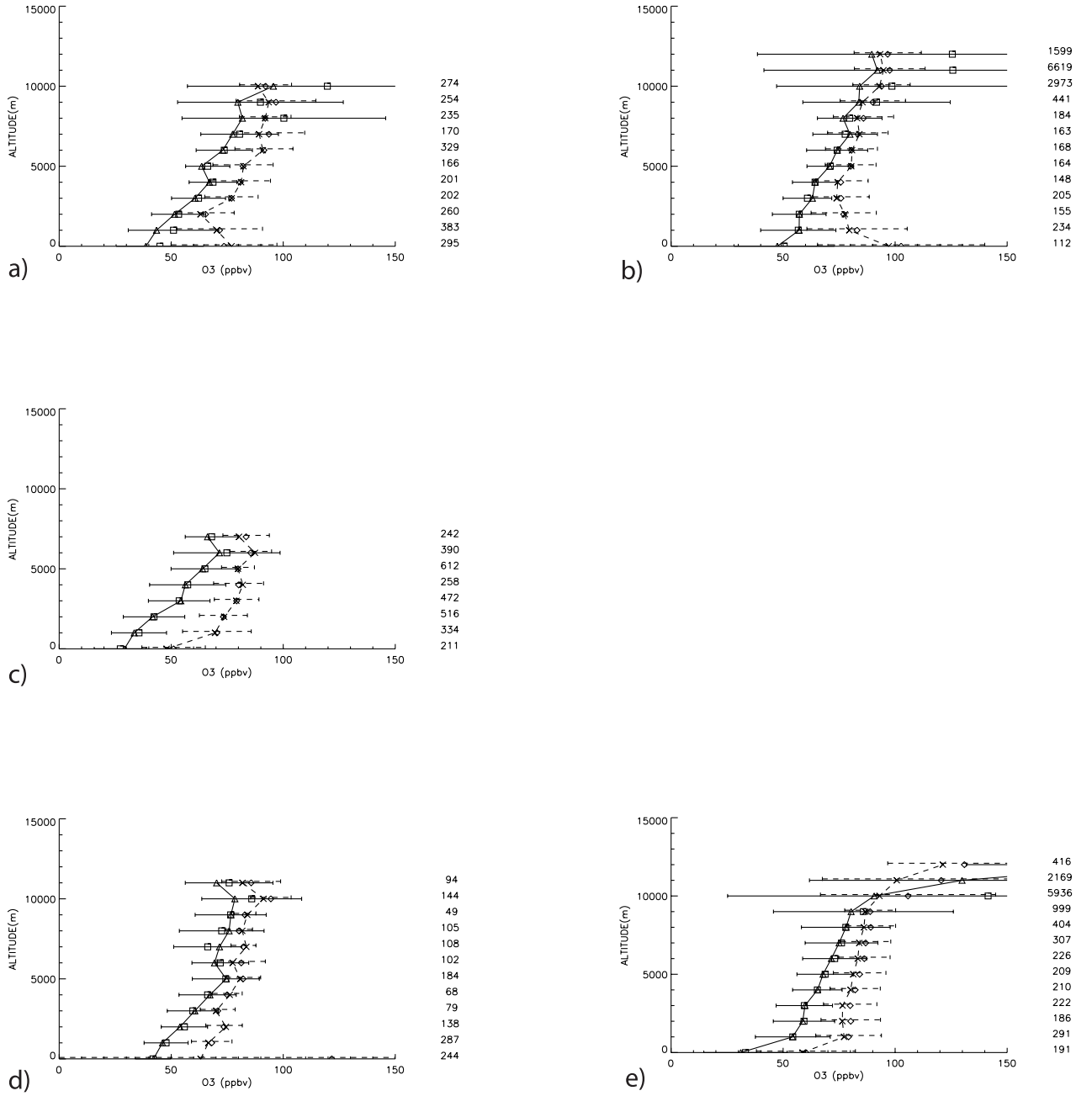

Figure 19. Same as Figure 3 but for O_3 (ppbv): (a) DC8, NEA domain; (b) MOZAIC, NEA domain; (c) BAE-146, NA domain; (d) FALCON, EU domain; and (e) MOZAIC, EU domain.

in the model would be useful as these sources are currently uncertain. Finally, further sensitivity studies to quantify the impact of North America wildfires on European air quality would be interesting.

[34] **Acknowledgments.** N.B., J.L.A., and V.H.P. acknowledge financial support from national programmes (PNCA, PATOM) provided by INSU, ADEME, Météo France, CNES as well as the Institut Geographique National (IGN) for hosting the DLR Falcon campaign at Creil, France. We also would like to thank the whole ICARTT team and, in particular, UK BAe-146 scientists (D. Stewart, G. Mills, L. Whalley, and J. R. Hopkins) and DC-8 scientists (P. Wennberg, R. Cohen, D. Blake, W. Brune, H. Singh, B. Heikes, and J. Barrick). We also express our gratitude to P. Nédélec and J. P. Cammas for provision of MOZAIC O_3 and CO data and to the NCAR MOPITT team for providing data. The National Center for Atmospheric Research is sponsored by the National Science Foundation. We are also grateful to E. Sternberg for her comments that significantly improved the manuscript.

References

Auvray, M., I. Bey, E. Llull, M. G. Schultz, and S. Rast (2007), A model investigation of tropospheric ozone chemical tendencies in long-range transported pollution plumes, *J. Geophys. Res.*, *112*, D05304, doi:10.1029/2006JD007137.

Barthe, C., J.-P. Pinty, and C. Mari (2007), Lightning-produced NO_x in an explicit electrical scheme tested in a Stratosphere-Troposphere Experiment: Radiation, Aerosols, and Ozone case study, *J. Geophys. Res.*, *112*, D04302, doi:10.1029/2006JD007402.

Bechtold, P., et al. (2001), A mass flux convection scheme for regional and global models, *Q. J. R. Meteorol. Soc.*, *127*, 869–886.

Bey, I., et al. (2001), Global modeling of tropospheric chemistry with assimilated meteorology: Model description and evaluation, *J. Geophys. Res.*, *106*(D19), 23,073–23,095.

Cook, P., et al. (2007), Forest fire plumes over the North Atlantic: p-TOMCAT model simulations with aircraft and satellite measurements from the ITOP/ICARTT Campaign, *J. Geophys. Res.*, *112*, D10S43, doi:10.1029/2006JD007563.

Courtier, P., et al. (1991), The ARPEGE project at Météo-France, in Workshop on Numerical Methods in *Atmopheric Models*, vol. 2, pp. 193–231, Eur. Cent. for Med.-Range Weather Forecasts, Reading, U. K.

Crowther, R. A., K. S. Law, J. A. Pyle, and S. Bekki (2002), Characterizing the effect of large-scale model resolution upon calculated OH production using MOZAIC data, *Geophys. Res. Lett.*, *29*(21), 1613, doi:10.1029/2002GL014660.

Damoah, R., N. Spichtinger, C. Forster, P. James, I. Mattis, U. Wandinger, S. Beirle, T. Wagner, and A. Stohl (2004), Around the world in 17 days—Hemispheric scale transport of forest fire smoke from Russia in May 2003, *Atmos. Chem. Phys.*, *4*, 1311–1321.

Damoah, R., N. Spichtinger, R. Servranckx, M. Fromm, E. W. Eloranta, I. A. Razenkov, P. James, M. Shulski, C. Forster, and A. Stohl (2006), A case study of pyro-convection using a transport model and remote sensing data, *Atmos. Chem. Phys.*, *6*, 173–185.

Decaria, A. J., et al. (2005), Lightning generated NO_x and its impact on tropospheric ozone production: A three-dimensional modeling study of a Stratospheric-Troposphere Experiment: Radiation, Aerosols and Ozone (STERAO-A) thunderstorm, *J. Geophys. Res.*, *110*, D14303, doi:10.1029/2004JD005556.

Deeter, N., et al. (2003), Operational carbon monoxide retrieval algorithm and selected result for the MOPITT instrument, *J. Geophys. Res.*, *108*(D14), 4399, doi:10.1029/2002JD003186.

Deeter, N., et al. (2004), Vertical resolution and information content of CO profiles retrieved by MOPITT, *Geophys. Res. Lett.*, *31*, L15112, doi:10.1029/2004GL020235.

Dentener, F., et al. (2004), The impact of air pollutant and methane emission controls on tropospheric ozone and radiative forcing: CTM calculations for the period 1990–2030, *Atmos. Chem. Phys.*, *4*, 1551–1564.

Dentener, F., et al. (2006), The global atmospheric environment for the next generation, *Environ. Sci. Technol.*, *40*(11), 3586–3594, doi:10.1021/es0523845.

Di Carlo, P., et al. (2004), Missing OH reactivity in a forest: Evidence for unknown reactive biogenic VOCs, *Science*, *304*(5671), 722–725, doi:10.1126/science.

Drummond, J. R., and G. S. Mand (1996), The Measurements of Pollution in the Troposphere (MOPITT) instrument: Overall performance and calibration requirements, *J. Atmos. Oceanic Technol.*, *13*, 314–320.

Emmons, L. K., et al. (2004), Validation of Measurements of Pollution in the Troposphere (MOPITT) CO retrievals with aircraft in situ profiles, *J. Geophys. Res.*, *109*, D03309, doi:10.1029/2003JD004101.

Fehsenfeld, F., et al. (2006), International Consortium for Atmospheric Research on Transport and Transformation (ICARTT): North America to Europe—Overview of the 2004 summer field study, *J. Geophys. Res.*, *111*, D23S01, doi:10.1029/2006JD007829.

Fiore, A. M., D. J. Jacob, I. Bey, R. M. Yantosca, B. D. Field, A. C. Fusco, and J. G. Wilkinson (2002), Background ozone over the United States in summer: Origin, trend, and contribution to pollution episodes, *J. Geophys. Res.*, *107*(D15), 4275, doi:10.1029/2001JD000982.

Fiore, A. M., et al. (2005), Evaluating the contribution of changes in isoprene emissions to surface ozone trends over eastern United States, *J. Geophys. Res.*, *110*, D12303, doi:10.1029/2004JD005485.

Frost, G. J., et al. (2002), Comparisons of box model calculations and measurements of formaldehyde from the 1997 North Atlantic Regional Experiment, *J. Geophys. Res.*, *107*(D8), 4060, doi:10.1029/2001JD000896.

Fuelberg, H. E., et al. (2007), Meteorological conditions and anomalies during the Intercontinental Chemical Transport Experiment–North America, *J. Geophys. Res.*, *112*, D12S06, doi:10.1029/2006JD007734.

Giorgi, F., and W. L. Chameides (1986), Rainout lifetimes of highly soluble aerosols and gases as inferred from simulations with a general circulation model, *J. Geophys. Res.*, *91*, 14,367–14,376.

Guenther, A., et al. (1995), A global model of natural volatile compound emissions, *J. Geophys. Res.*, *100*, 8873–8892.

Heland, J., et al. (2003), Aircraft measurements of nitrogen oxides, ozone, and carbon monoxide during MINOS 2001: Distributions and correlation analyses, *Atmos. Chem. Phys. Disc.*, *3*, 1991–2026.

Höller, H., et al. (1999), Lightning produced NOx (LINOX): Experiment design and case study results, *J. Geophys. Res.*, *104*(D11), 13,911–13,922.

Horowitz, L. W., et al. (2003), A global simulation of tropospheric ozone and related tracers: Description and evaluation of MOZART, version 2, *J. Geophys. Res.*, *108*(D24), 4784, doi:10.1029/2002JD002853.

Hudman, R. C., et al. (2004), Ozone production in transpacific Asian pollution plumes and implications for ozone air quality in California, *J. Geophys. Res.*, *109*, D23S10, doi:10.1029/2004JD004974.

Huntrieser, H., et al. (1998), Transport and production of NOx in electrified thunderstorm: Survey of previous studies and new observations at midlatitudes, *J. Geophys. Res.*, *103*(D21), 28,247–28,264.

Husar, R. B., et al. (2001), Asian dust events of April 1998, *J. Geophys. Res.*, *106*, 18,317–18,330.

Jaffe, D., et al. (1999), Transport of Asian air pollution to North America, *Geophys. Res. Lett.*, *26*, 711–714.

Jang, J.-C., H. E. Jeffries, and S. Tonnesen (1995), Sensitivity of ozone to model grid resolution. II: Detailed processe analysis for ozone chemistry, *Atmos. Environ.*, *29*, 3101–3114.

Josse, B., P. Simon, and V.-H. Peuch (2004), Radon global simulations with the multiscale chemistry transport model MOCAGE, *Tellus, Ser. B*, *56*, 339–356.

Law, K., et al. (2000), Comparisons between global chemistry transport model results and Measurements of Ozone and Water Vapor by Airbus In-Service Aircraft (MOZAIC) data, *J. Geophys. Res.*, *105*(D1), 1503–1525.

Lefèvre, F., et al. (1994), The 1991–1992 stratospheric winter: Three-dimensional simulations, *J. Geophys. Res.*, *99*, 8183–8195.

Liu, H., D. J. Jacob, I. Bey, and R. M. Yantosca (2001), Constraints from ^{210}Pb and ^{7}Be on wet deposition and transport in a global three-dimensional chemical-transport model driven by assimilated meteorological fields, *J. Geophys. Res.*, *106*, 12,109–12,128.

Louis, J.-F. (1979), A parametric model for vertical eddy-fluxes in the Atmosphere, *Boundary Layer Meteorol.*, *17*, 187–202.

Marenco, A., et al. (1998), Measurement of ozone and water vapor by Airbus in-service aircraft: The MOZAIC airborne program, An overview, *J. Geophys. Res.*, *103*(D19), 25,631–25,642.

Mari, C., D. J. Jacob, and P. Bechtold (2000), Transport and scavenging of soluble gases in a deep convective cloud, *J. Geophys. Res.*, *105*, 22,255–22,267.

Mari, C., J. P. Chaboureau, J. P. Pinty, J. Duron, P. Mascart, J. P. Camas, and F. Gheusi (2006), Regional lightning NOx sources during the TROCCINOX experiment, *Atmos. Chem. Phys.*, *6*, 5559–5572.

Martin, R. V., et al. (2003), Global and regional decreases in tropospheric oxidant from photochemical effects of aerosols, *J. Geophys. Res.*, *108*(D3), 4097, doi:10.1029/2002JD002622.

McKendry, I. G., J. P. Hacker, R. Stull, S. Sakiyama, D. Mignaca, and K. Reid (2001), Long-range transport of Asian dust to Lower Fraser Valley, British Columbia, Canada, *J. Geophys. Res.*, *106*, 18,361–18,370.

Mena-Carrasco, M., et al. (2007), Improving regional ozone modeling through systematic evaluation of errors using the aircraft observations during ICARTT, *J. Geophys. Res.*, doi:10.1029/2006JD007762, in press.

Methven, J., et al. (2006), Establishing Lagrangian connections between observations within air masses crossing the Atlantic during ICARTT experiment, *J. Geophys. Res.*, *111*, D23S62, doi:10.1029/2006JD007540.

Michou, M., and V.-H. Peuch (2002), Surface exchanges in the MOCAGE multi-scale chemistry and transport model, *J. Water Sci*, *15*, 173–204.

Michou, M., et al. (2005), Measured and modeled dry deposition velocities over the ESCOMPTE area, *Atmos. Res*, *74*(1–4), 89–116.

Nédélec, P., et al. (2003), An improved infrared carbon monoxide analyser for routine measurements aboard commercial aircraft: Technical validation and first scientific results of the MOZAIC III programme, *Atmos. Chem. Phys.*, *3*, 1551–1564.

Neuman, J. A., et al. (2006), Reactive nitrogen transport and photochemistry in urban plumes over the North Atlantic Ocean, *J. Geophys. Res.*, *111*, D23S54, doi:10.1029/2005JD007010.

Nho-Kim, E.-Y., et al. (2004), Parameterization of size dependent particle dry deposition velocities for global modeling, *Atmos. Environ.*, *38*(13), 1933–1942.

Pfister, G., et al. (2005), Quantifying CO emissions from the 2004 Alaskan wildfires using MOPITT CO data, *Geophys. Res. Lett.*, *32*, L11809, doi:10.1029/2005GL022995.

Richter, A., and J. P. Burrows (2002), Retrieval of tropospheric NO_2 from GOME measurements, *Adv. Space Res.*, *29*(11), 1673–1683.

Savage, N. H., K. S. Law, J. A. Pyle, A. Richter, and J. P. Burrows (2004), Using GOME NO_2 satellite data to examine regional differences in TOMCAT model performance, *Atmos. Chem. Phys.*, *4*, 1895–1912.

Singh, H. B., W. H. Brune, J. H. Crawford, D. J. Jacob, and P. B. Russell (2006), Overview of the summer 2004 Intercontinental Chemical Transport Experiment-North America (INTEX-A), *J. Geophys. Res.*, *111*, D24S01, doi:10.1029/2006JD007905.

Singh, H. B., et al. (2007), Reactive nitrogen distribution and partitioning in the North American troposphere and lowermost stratosphere, *J. Geophys. Res.*, *112*, D12S04, doi:10.1029/2006JD007664.

Stockwell, W. R., et al. (1997), A new mechanism for regional atmospheric chemistry modelling, *J. Geophys. Res.*, *102*(D22), 25,847–25,879.

Thouret, V., et al. (1998), Comparisons of ozone measurements from the MOZAIC airborne programme and the ozone sounding network at eight locations, *J. Geophys. Res.*, *103*, 25,695–25,720.

Trickl, T., O. R. Cooper, H. Eisele, P. James, R. Mucke, and A. Stohl (2003), Intercontinental transport and its influence on the ozone concentrations over the central Europe: Three case studies, *J. Geophys. Res.*, *108*(D12), 8530, doi:10.1029/2002JD002735.

Turquety, S., et al. (2007), Inventory of boreal fire emissions for North America in 2004: Importance of peat burning and pyroconvective injection, *J. Geophys. Res.*, *112*, D12S03, doi:10.1029/2006JD007281.

Vandeirmeiren, K., et al. (2005), Impact of rising tropospheric ozone on potato: Effects on photosynthesis, growth, productivity and yield quality, *Plant Cell Environ.*, *28*, 982–996.

Wang, Y., et al. (1998), Global simulation of tropospheric O_3-NO_x-hydrocarbon chemistry: 2. Model evalution and global ozone budget, *J. Geophys. Res.*, *103*(D9), 10,727–10,755.

Wesely, M. L. (1989), Parameterization of surface resistances to gaseous dry deposition in regional-scale numerical models, *Atmos. Environ.*, *23*, 1293–1304.

Wild, O., K. S. Law, D. S. McKenna, B. J. Bandy, S. A. Penkett, and J. A. Pyle (1996), Photochemical trajectory modeling studies of the North Atlantic region during August 1993, *J. Geophys. Res.*, *101*, 29,269–29,288.

Wilkening, K. E., L. A. Barrie, and M. Engle (2000), Transpacific air pollution, *Science*, *290*, 65–67.

S. R. Arnold, Institute for Atmospheric Science, School of Earth and Environment, University of Leeds, Leeds LS2 9JT, UK.

J. L. Attié, B. Barret, N. Bousserez, and C. Mari, OMP (Laboratoire d'Aérologie), 14 avenue Edouard Belin, F-31400 Toulouse, France. (attjl@aero.obs-mip.fr)

M. Avery, E. V. Browell, J. W. Hair, and G. Sachse, NASA Langley Research Center, Mail Stop 401B, 5 North Dryden Street, Hampton, VA 23681-2199, USA.

D. Edwards, L. Emmons, and G. Pfister, National Center for Atmospheric Research, Boulder, CO 80307, USA.

A. Heckel and A. Richter, Institute of Environmental Physics, D-28334 Bremen, Germany.

A. Lewis, Department of Chemistry, University of York, York YO10 5DD, UK.

M. Michou and V. H. Peuch, Centre National de Recherches Météorologiques/Météo France, F-31057 Toulouse, France.

H. Schlager, Institut für Physik der Atmosphäre, Deutsches Zentrum für Luft- und Raumfahrt, Operpfaffenhofen, D-82230 Wessling, Germany.